Mesoscale eddy parameterization in an energetically constrained way using a state estimation

Yongsu NA
PhD student (ynaab@connect.ust.hk)
Ocean Modelling and Fluids Group

Contents

1. Eddy parameterization
(1) Eddies and turbulence

Eddies: Identifiable (spinning) structures in turbulent flows.

- Turbulence -

- In Ocean & Atmosphere: affects mass, momentum, energy, and tracer transport.
- Uneasy to define mathematically.

- Some general characteristics
    - irregular, chaotic, and unpredictable with fluctuationing fields.
    - enhances nonlinearity of the flow.
    - streaks and swirls that deform, spin, merge, and divide.
    - mixing and diffusion of mass, momentum, heat, and tracers.
    - dissipates as energy transfers to smaller scales and converts to heat.

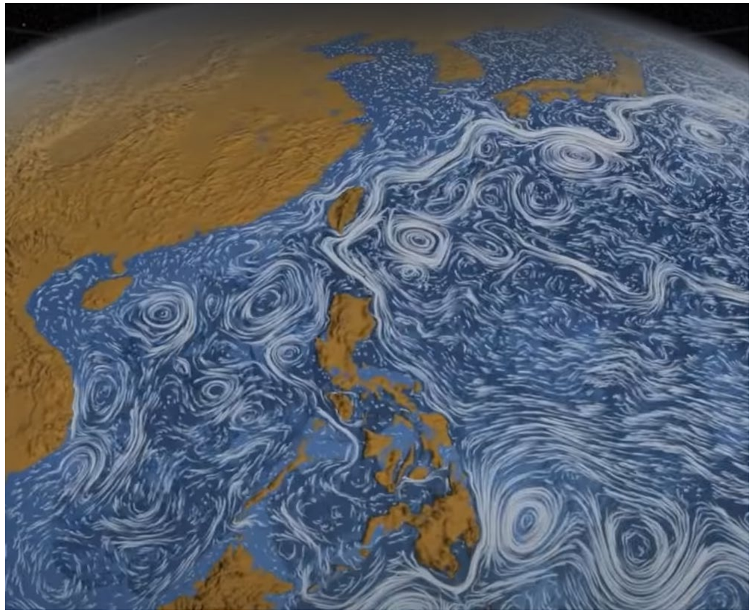

Fig.1 Oceanic eddies
(obtained from the ECCO state estimate)

- Reynolds number (Re) can be used as a proxy for assessing if a flow is laminar/turbulent.

- Flows with high Reynolds number are usually turbulent, given that the turbulence enhances advection.

$$\frac{inertial\ term}{viscous\ term} = \frac{U^2/L}{\nu U/L^2} = \frac{UL}{\nu}, \qquad Re \equiv \frac{UL}{\nu}$$

- Momentum equation: for momentum conservation

$$\frac{\partial \boldsymbol{v}}{\partial t} + (\boldsymbol{v} \cdot \nabla)\boldsymbol{v} + 2\boldsymbol{\Omega} \times \boldsymbol{v} = -\frac{1}{\rho}\nabla p + \nu\nabla^2\boldsymbol{v} + \boldsymbol{g}$$

inertial (or advective) term: $(\boldsymbol{v} \cdot \nabla)\boldsymbol{v}$

viscous term: $\nu\nabla^2\boldsymbol{v}$

- Ocean (with the scale of our interest) is turbulent.

using

$$U = 0.1ms^{-1},$$

$$L = 100km,$$

$$\nu = 10^{-6}m^2s^{-1}$$

$$Re = \frac{inertial\ term}{viscous\ term} \approx 10^{10}$$

The viscous term is negligible as the ‘nonlinear’ inertial term dominates.

- Equations of motion (Navier-Stokes equations)

  - Mass continuity equation: for mass conservation

$$\frac{\partial \rho}{\partial t} + \nabla \cdot (\rho \boldsymbol{v}) = 0$$

  - Momentum equation: for momentum conservation

$$\frac{\partial \boldsymbol{v}}{\partial t} + (\boldsymbol{v} \cdot \nabla)\boldsymbol{v} + 2\boldsymbol{\Omega} \times \boldsymbol{v} = -\frac{1}{\rho}\nabla p + \nu \nabla^2 \boldsymbol{v} + \boldsymbol{g}$$

  - Equation of state: describes the state of a system in equilibrium

$$\frac{1}{\rho} = \frac{1}{\rho_0}\left[1 + \beta_T(1 + \gamma^* p)(T - T_0) + \frac{{\beta_T}^*}{2}(T - T_0)^2 - \beta_S(S - S_0) - \beta_p(p - p_0)\right]$$

  - Thermodynamic equation: for energy conservation

$$\frac{DI}{Dt} + \frac{p}{\rho}\nabla \cdot \boldsymbol{v} = \dot{Q}_{\boldsymbol{E}}$$

- *Ocean modelling is based on the equations of motion.*
- *Difficulty obtaining analytic solutions due to nonlinearity.*
- *Alternative: approximate solutions from numerical simulations.*

1. Eddy parameterization

(4) Need for parameterizing sub-grid processes

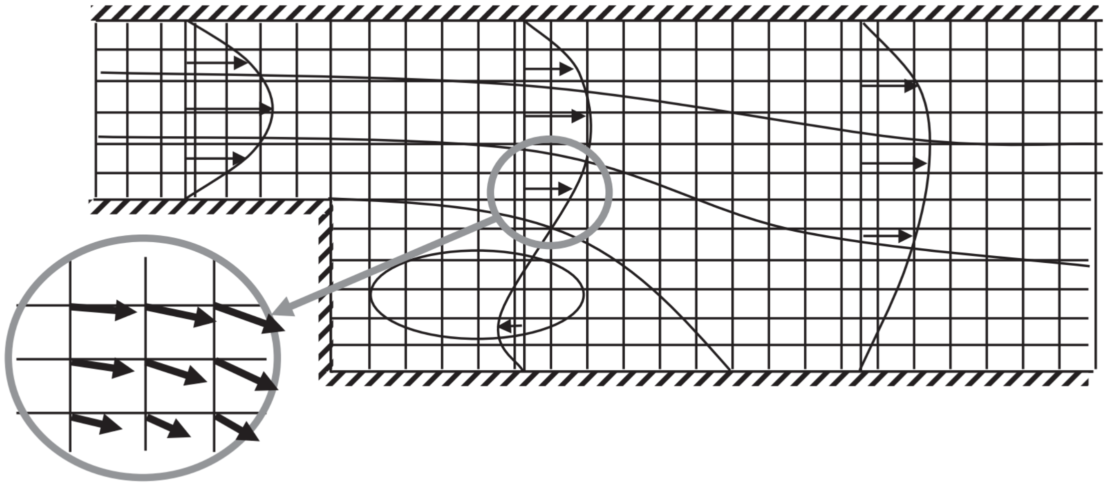

Fig.2 The approximation of a flow field on a discrete grid

- Spatial and temporal Discretization of numerical simulations in essence and due to computational limit.
- Sub-grid processes need to be parameterized.

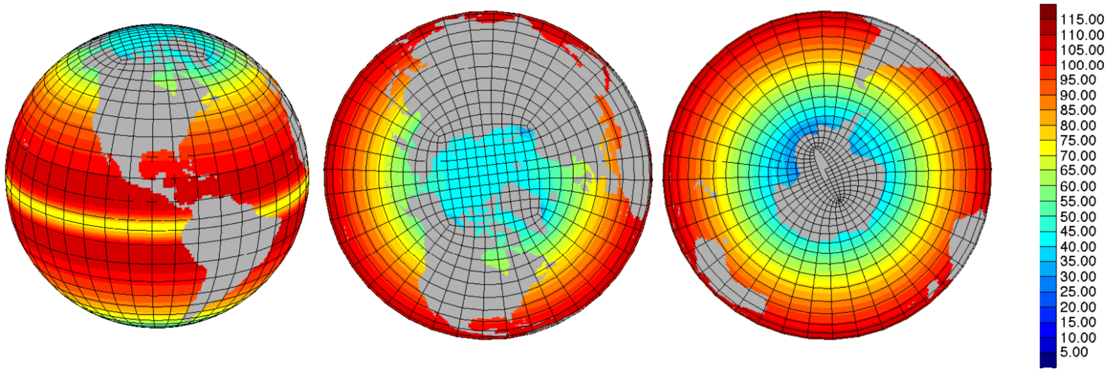

Fig.3 LLC90 grid spacing (in km) used in ECCO

(e.g.) ECCO: a simulation (or reanalysis) of the global ocean.

- Grid resolution: a nominal 1° (≈ 100 km at mid latitudes).
- Cannot resolve mesoscale eddies (its cut-off is roughly 10 km).
- Uses Gent-McWilliams (GM) scheme to parameterize it.

1D equation for advection and diffusion
of a conserved quantity phi in an incompressible fluid

$$\frac{\partial \varphi}{\partial t} + (\boldsymbol{v} \cdot \nabla)\varphi = \kappa \nabla^2 \varphi$$

Apply Reynolds-averaging
(separate fluctuations from time-mean quantities)

$$\frac{\partial \bar{\varphi}}{\partial t} + (\boldsymbol{v} \cdot \nabla)\bar{\varphi} = \nabla \cdot (\overline{\boldsymbol{v}'\varphi'}) + \kappa \nabla^2 \bar{\varphi}$$

bar: time-mean
prime: fluctuation

Apply turbulent diffusivity hypothesis

$$\varphi' = -l' \frac{\partial \bar{\varphi}}{\partial x} - \frac{1}{2} l'^2 \frac{\partial^2 \bar{\varphi}}{\partial x^2} + O(l'^3)$$

- Knowledge from experiments
  : eddy-induced advection resembles molecular diffusion in that they are down-gradient.

The fluctuation term $\overline{\boldsymbol{v}'\varphi'}$ becomes $-\overline{v_i' l_j'}\partial_j \bar{\varphi} = -K_{ij}\partial_j \bar{\varphi}$ with eddy diffusivity tensor $\boldsymbol{K} = K_{ij} \equiv \overline{v_i' l_j'}$

- Note: It is enhanced advection due to eddies.
  The name is from its similarity with molecular diffusion.

Molecular diffusion $\kappa \nabla^2 \bar{\varphi}$ is neglected as eddies dominate it,
and the main issue becomes assigning an adequate value to $\boldsymbol{K}$

$$\frac{\partial \bar{\varphi}}{\partial t} + (\boldsymbol{v} \cdot \nabla)\bar{\varphi} = \nabla \cdot (\boldsymbol{K} \nabla \bar{\varphi})$$

2. Eddy parameterization
(6) GM and GEOMETRIC

Gent-McWilliams (GM) scheme has weakness in representing

- Eddy saturation
  : lack of sensitivity of the Southern Ocean circumpolar transport to changing wind forcing

- Eddy compensation
  : reduced sensitivity of the time-mean residual meridional overturning circulation to changing wind forcing

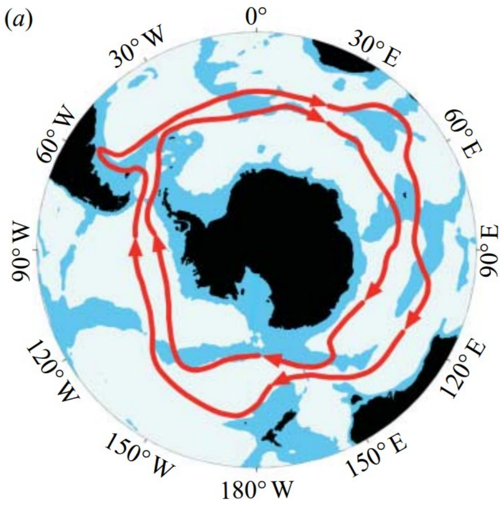

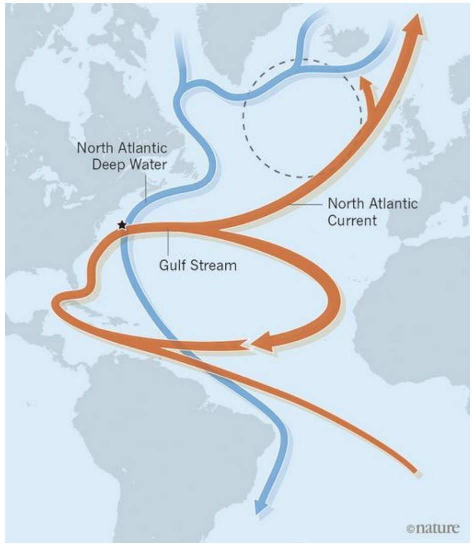

Geometry and Energetics of Ocean Mesoscale Eddies and Their Rectified Impact on Climate (GEOMETRIC) scheme

- Energetic approach which is still based on GM

- uses eddy energy budget equation

$$\frac{\partial}{\partial t}\int E\,dz + \nabla_H \cdot \left[(\tilde{\boldsymbol{u}}^z - |c|\boldsymbol{e}_x)\int E\,dz\right] = \int \kappa_{gm}\frac{M^4}{N^2}dz - \lambda\int E\,dz + \eta_E {\nabla^2}_H \int E\,dz$$

advection　　source　　dissipation　　diffusion

Computational fluid dynamics (CFD) emerged in the late 1950s and has rapidly developed since 1970s.

- Numerical simulations - based on the theories of geophysical fluid dynamics
- Comparison between 'modelling outputs' and 'observations' → Improvement in theories.

- We may tune model parameters to make modelling outputs as close as possible to observations (infer a&b in y'=ax+b given y).

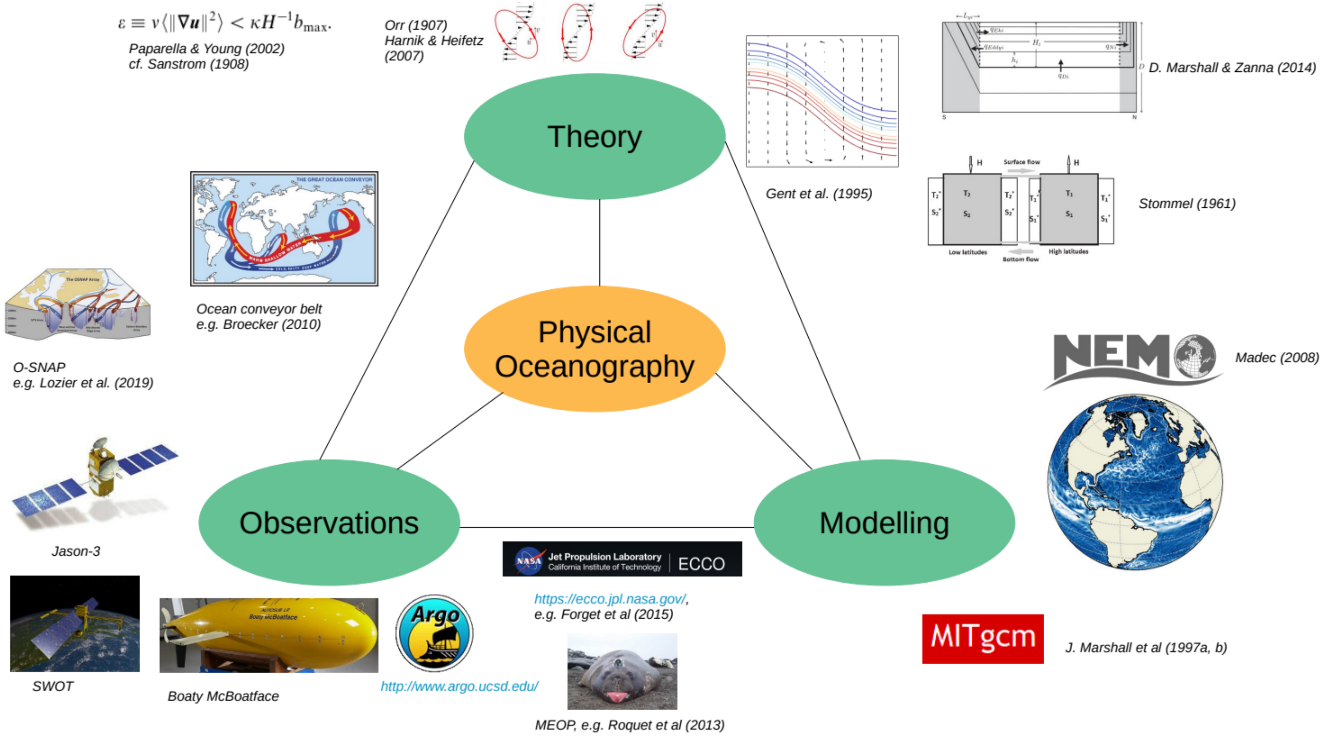

Fig.4 Components of physical oceanography

A basic way of tunning parameters

: Repeat tuning & modelling until outputs at the end of the simulation become sufficiently close to observations.

- It is intuitive and easy, but is not adequate for parameter inference.

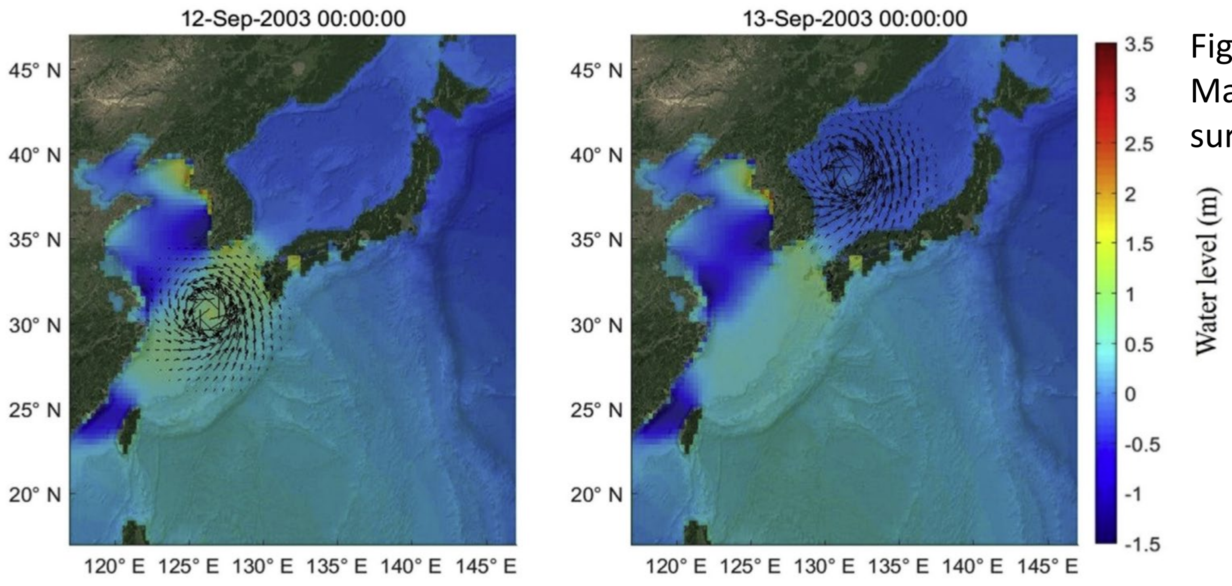

Fig.5 Wind field of Typhoon Maemi (2003) and sea surface height (SSH).

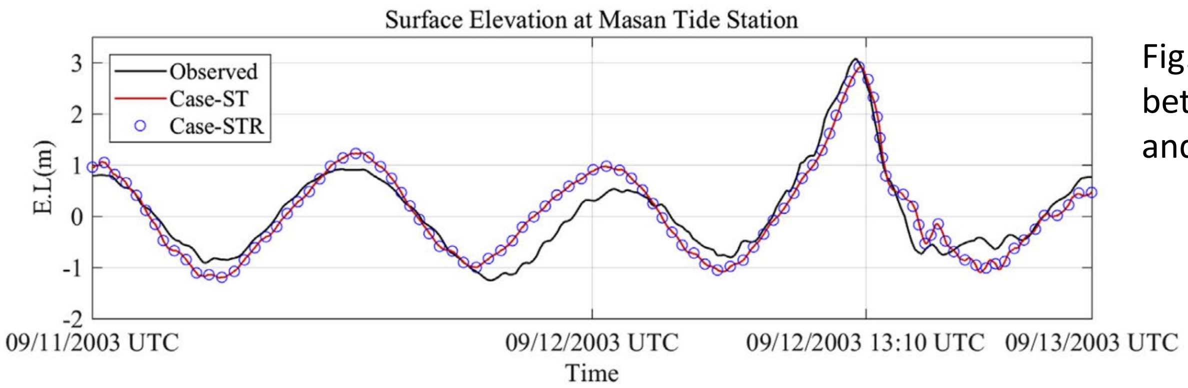

Fig.6 SSH comparison between a simulation and observations.

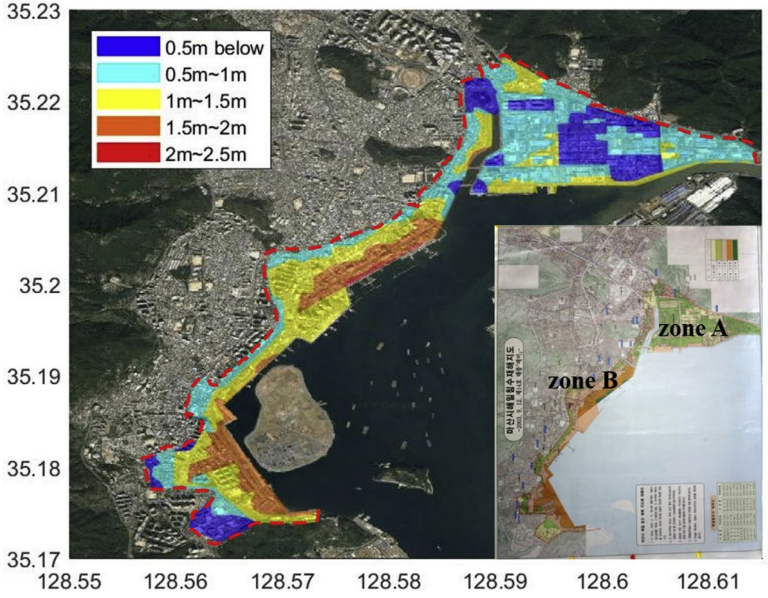

Fig.7 Flood area comparison between a simulation and observations.

Baseball as an example of numerical simulations.

- Assume ‘a pitcher and a ball he throws’ is the real-world oceanic system, then the recorded trajectory of the ball could be seen as ocean observations.

- We want to make a machine (model) that mimic the pitcher and the ball (oceanic system).

Fig.8 A pitcher and a ball that could be seen as the real-world oceanic system.

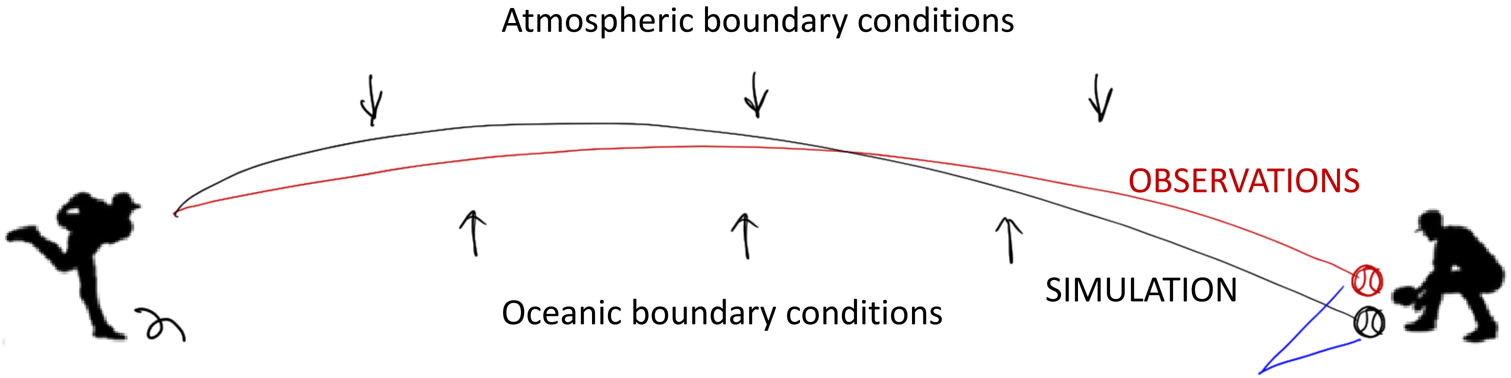

MODEL
- Physics
- Numerical schemes
- Parameters
- Initial conditions

COMPARISON at the end
↓
Tune the parameters
↓
Run the model again

Called a machine-gun, trial and error, or gradient-free approach

Problems of the basic way of tunning parameters (comparison at the end)

Problem 1: Possibility of dynamical inconsistency

PB2: Possibility of unphysical tuning

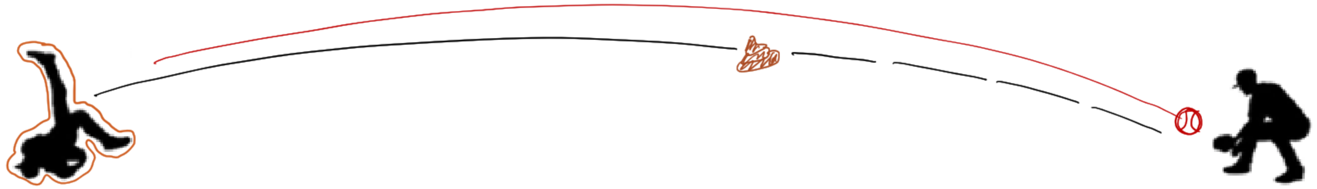

PB3: Computational cost
(ECCO forward run takes 12~24 hours, while forward+adjoint run takes 5~6 days (using HKUST HPC3 96 cores))

PB4: A number of parameters & oceanic/atmospheric forcings (can be t-dep. or 3D) should be optimized together.

State estimation is a better optimization over the **machine-gun approach** because it is

1. Dynamically consistent
   : comparison between observations and a simulation along the entire trajectory, not at the end only.

2. Driven by mathematical rules
   : parameters are tuned by setting up a cost function and control variables, not arbitrarily.

3. Gradient-based
   : efficient way of searching the optimum iteratively as it uses mathematical information dJ/dm.

4. Correcting parameters and forcings at the same time
   : by assigning them as controls.

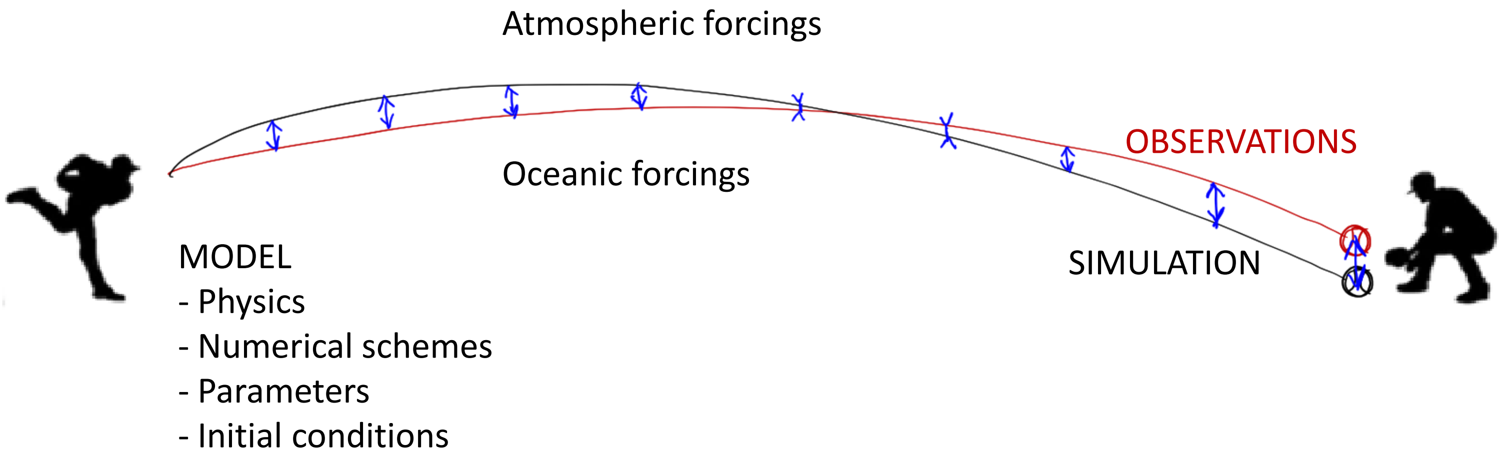

A simple case of linear regression: Temperature over time at a fixed location

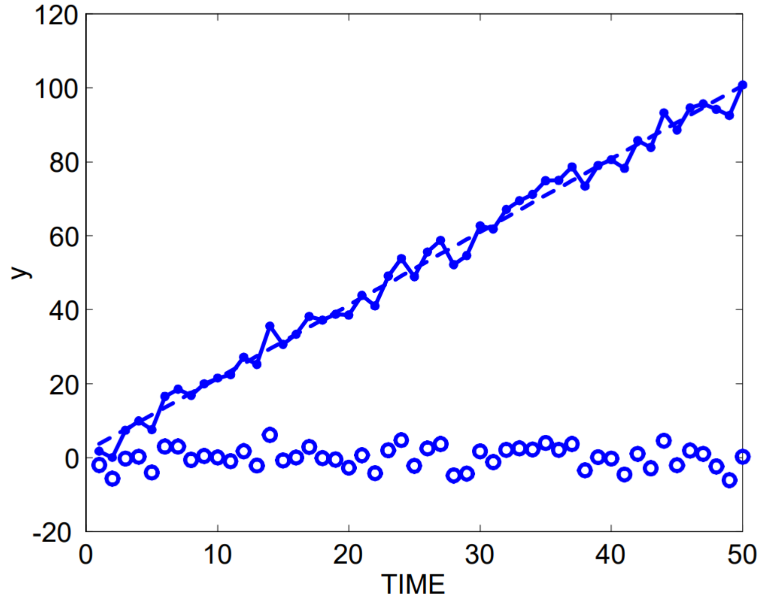

- Dashed line: our understanding of a system (i.e. theory, model)
  - $\theta(t) = a + bt$
  - We believe that the temperature linearly increases over time
- Dots connected with a solid line: measurements
  - $y(t_i) = \theta(t_i) + n(t_i) = a + bt_i + n(t_i)$
- $n(t_i)$ (Open circles)
  : noises of the measurements compared to the model after fixing a and b

In a matrix form, $\boldsymbol{Ex} + \boldsymbol{n} = \boldsymbol{y}$ or simply $\boldsymbol{Ex} \sim \boldsymbol{y}$

$$\boldsymbol{E} = \begin{pmatrix} 1 & t_1 \\ 1 & t_2 \\ \cdot & \cdot \\ \cdot & \cdot \\ 1 & t_M \end{pmatrix}, \quad \boldsymbol{x} = \begin{bmatrix} a \\ b \end{bmatrix}, \quad \boldsymbol{y} = \begin{bmatrix} y(t_1) \\ y(t_2) \\ \cdot \\ \cdot \\ y(t_M) \end{bmatrix}, \quad \boldsymbol{n} = \begin{bmatrix} n(t_1) \\ n(t_2) \\ \cdot \\ \cdot \\ n(t_M) \end{bmatrix}$$

We want to obtain an optimal solution by combining our model and measurements.

That is, we will tune the coefficients a and b to minimize the noise.

We want to obtain an optimal solution by combining our model and measurements.
That is, we will tune the coefficients a and b to minimize the noise.

$$y(t_i) = \theta(t_i) + n(t_i) = a + bt_i + n(t_i)$$

$$\boldsymbol{E} = \begin{Bmatrix} 1 & t_1 \\ 1 & t_2 \\ \cdot & \cdot \\ \cdot & \cdot \\ 1 & t_M \end{Bmatrix}, \quad \boldsymbol{x} = \begin{bmatrix} a \\ b \end{bmatrix}, \quad \boldsymbol{y} = \begin{bmatrix} y(t_1) \\ y(t_2) \\ \cdot \\ \cdot \\ y(t_M) \end{bmatrix}, \quad \boldsymbol{n} = \begin{bmatrix} n(t_1) \\ n(t_2) \\ \cdot \\ \cdot \\ n(t_M) \end{bmatrix}$$

In a matrix form, $\boldsymbol{Ex} + \boldsymbol{n} = \boldsymbol{y}$ or simply $\boldsymbol{Ex} \sim \boldsymbol{y}$

- First, we set a cost function
  which is the sum of squared noise at every timestep.

$$J = \sum_{i=1}^{M} {n_i}^2 = \boldsymbol{n}^T\boldsymbol{n} = (\boldsymbol{y} - \boldsymbol{Ex})^T(\boldsymbol{y} - \boldsymbol{Ex}) = \sum_{i=1}^{M} (y_i - a - bt_i)^2$$

- Then our goal becomes minimizing J and it is where $dJ = 0$

$$dJ = \sum_i \frac{\partial J}{\partial x_i} dx_i = \left(\frac{\partial J}{\partial \boldsymbol{x}}\right)^T d\boldsymbol{x} = 2d\boldsymbol{x}^T(\boldsymbol{E}^T\boldsymbol{y} - \boldsymbol{E}^T\boldsymbol{Ex}) = 0$$

- To satisfy $dJ = 0$, $\boldsymbol{E}^T\boldsymbol{y} - \boldsymbol{E}^T\boldsymbol{Ex} = 0$ in other words $\boldsymbol{E}^T\boldsymbol{Ex} = \boldsymbol{E}^T\boldsymbol{y}$

- Assume that $\boldsymbol{E}^T\boldsymbol{E}$ has inverse. We can get an estimate of the solution $\tilde{\boldsymbol{x}} = (\boldsymbol{E}^T\boldsymbol{E})^{-1}\boldsymbol{E}^T\boldsymbol{y}$

3. State estimation
(6) ECCO compared to simple linear regression

Estimating the Circulation and Climate of the Ocean (ECCO) v4r3

- is a global ocean state estimate (or a reanalysis dataset) for a period from 1992 to 2015
- is produced by running MIT General Circulation Model (MITgcm)
- ran 59 forward/adjoint model iterations (together with gradient-based optimization)

ECCO is different in that…

- MODEL *(Instead of linear equation)*
  : The governing equations of motion and numerical schemes.

- OBSERVATIONS *(Instead of 1D temperature over time)*
  : Various oceanic & atmospheric observations and some of them are 3D and/or time-dependent.

- SUBJECTS *(Instead of a & b)*
  : Multiple parameters and oceanic & atmospheric forcings to be optimized together.

- OPTIMIZATION *(Instead of multiplying $(\boldsymbol{E}^T\boldsymbol{E})^{-1}$ to get $\tilde{\boldsymbol{x}}$)*
  : Gradient-based optimization that requires $dJ/d\boldsymbol{m}$.

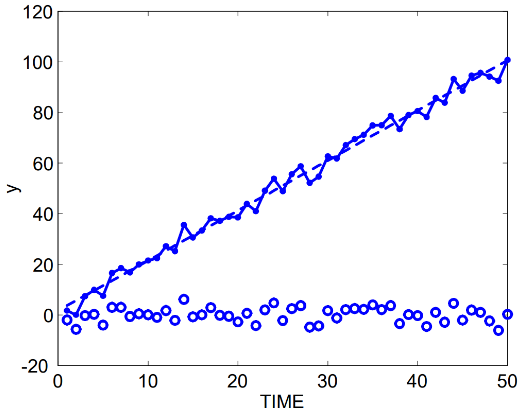

(5) ECCO's cost function and controls

$$m_i = SDM(\mathrm{u})$$

- m_i: model outputs
- S: subsampling or averaging
- D: diagnostics
- M: modelling
- u: controls

FORWARD RUN

$$d_i = P(m_i - o_i)$$

- d_i: raw model-data misfits
- P: post-processor
- m_i: model outputs
- o_i: data

$$J(\mathrm{u}) = \sum_i \left(d_i^T \boldsymbol{R}_i^{-1} d_i\right) + \sum_j \left(\mathrm{u}_j^T \mathrm{u}_j\right)$$

- $J(\mathrm{u})$: a squared model-data distance (J)
- d_i: a set of model-data misfits
- u_j: a set of non-dimensional controls

UPDATE

ADJOINT RUN

- Backward simulation carrying mismatch information.
- Produces dJ/dm at the end.

Gradient-based optimization

- Uses dJ/dm.
- Tells what to update.

Variable	Description	Period	Origin
MDT	DNSC08 mean SSH minus EGM2008 geoid model	1993–2004	Andersen and Knudsen (2009), Pavlis et al. (2012)
T, S	Blended monthly climatology		
	OCCA	2004–2006	Forget (2010)
	WOA 2005	Unclear	Locarnini et al. (2006)
	PHC 3.0	Unclear	Updated: Steele et al. (2001)
SLA	Daily bin average of along-track altimetry	1992–2011	Scharroo et al. (2004)
SST	Monthly maps	1992–2011	Reynolds et al. (2002)
ICF	Monthly maps	1992–2010	Comiso (1999)

Table 1. Gridded observations to which ECCO is constrained.

Data set	Origin
Argo	IFREMER
CTD	NODC, WOA09
XBT	NODC, WOA09
ITP	Toole et al. (2011)
SEaOS	Roquet et al. (2011)
bobbers	D. Fratantoni, CLIMODE
CTD	L. Talley, CLIMODE

Table 2. In situ temperature & salinity observations.

Description
Initial condition for temperature
Initial condition for salinity
Diapycnal diffusivity
Isopycnal diffusivity
GM intensity
Atmospheric temperature at 2 m
Specific humidity at 2 m
Precipitation
Downward longwave radiation
Downward shortwave radiation
Zonal wind stress
Meridional wind stress

Table 3. Control parameters and forcings of ECCO.

Geometry and Energetics of Ocean Mesoscale Eddies and Their Rectified Impact on Climate (GEOMETRIC) scheme

- Energetic approach which is still based on GM
- uses eddy energy budget equation

eddy dissipation coefficient

$$\frac{\partial}{\partial t}\int E\,dz + \nabla_H \cdot \left[(\tilde{\boldsymbol{u}}^z - |c|\boldsymbol{e}_x)\int E\,dz \right] = \int \kappa_{gm}\frac{M^4}{N^2}dz - \lambda\int E\,dz + \eta_E {\nabla^2}_H \int E\,dz$$

advection source dissipation diffusion

Description
Initial condition for temperature
Initial condition for salinity
Diapycnal diffusivity
Isopycnal diffusivity
GM intensity
Atmospheric temperature at 2 m
Specific humidity at 2 m
Precipitation
Downward longwave radiation
Downward shortwave radiation
Zonal wind stress
Meridional wind stress

Table 3. Control parameters and forcings of ECCO.

The effect of Monsoon winds to the South China Sea Sandwiched circulation

Yongsu NA
PhD student (ynaab@connect.ust.hk)
Department of Ocean Science
Ocean Modelling and Fluids Group

Contents

1. South China Sea (SCS) topography

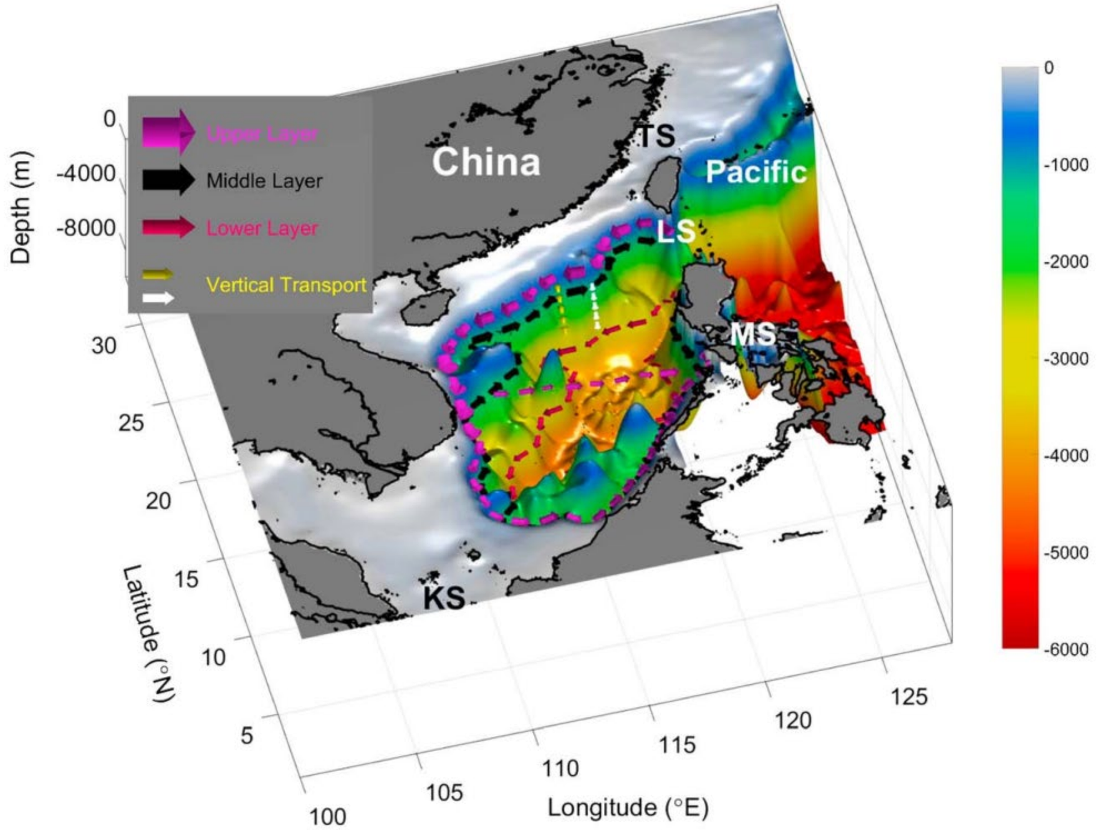

Fig.1 Schematic annual mean CAC circulation, based on Stokes's Theorem [Cai and Gan, 2019].

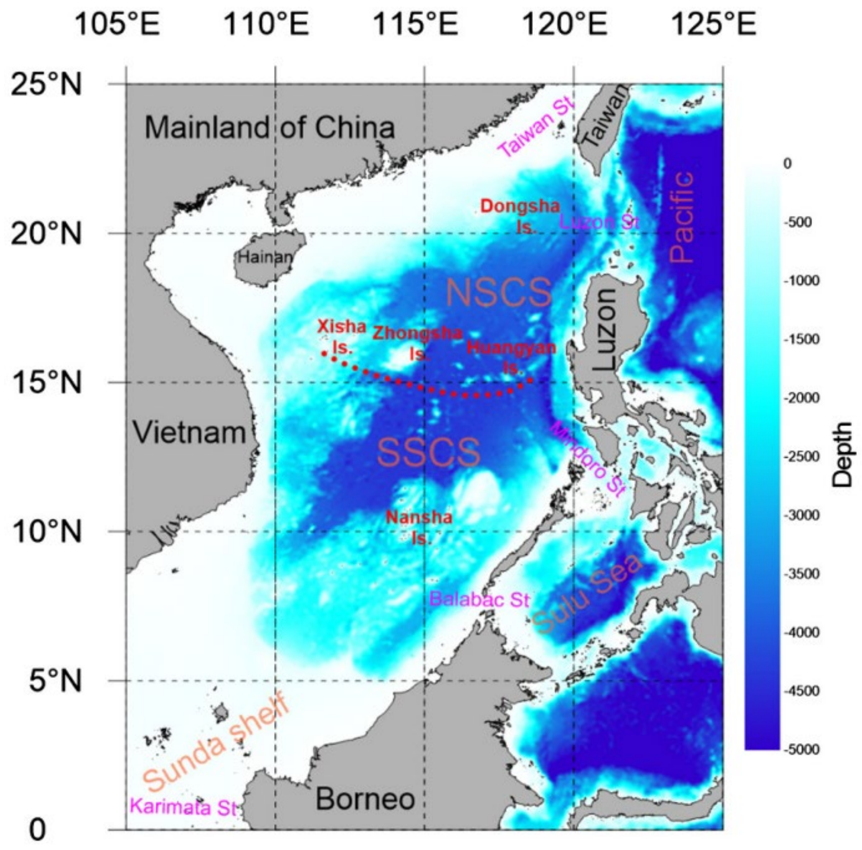

Fig.2 Topography of the SCS. The red dots indicate islands and seamounts [Zhu et al., 2019].

- Maximum depth: 5559 m
- Continental shelves: shallower than 100 m
- A chain of islands and seamounts
  : separates the basin into the NSCS and SSCS.

- Sill depth of straits
  - Luzon Strait: ~2000m
  - Mindoro Strait: ~400m
  - Taiwan, Karimata and Balabac Straits: < 100 m

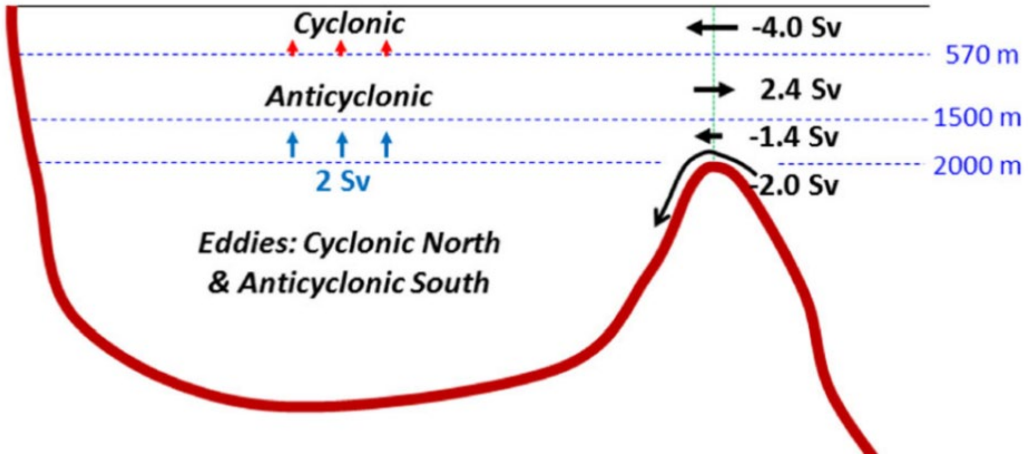

Fig.3 Modeled transport values across the Luzon Strait and the resulting upwelling [Xu and Oey, 2014].

- Upper L (~500m): westward intrusion of Kuroshio WBC
- Intermediate L (500~1700m): compensatory eastward countercurrents
- Deep L (1700m~): westward deepwater overflow from Western Pacific
- rough topography
  → energetic internal tides, internal waves and mesoscale eddies
  → enhanced abyssal diapycnal mixing
  → more vertically homogenous than WP counterpart
  → opposite density gradients across Luzon Strait at inter. & deep L

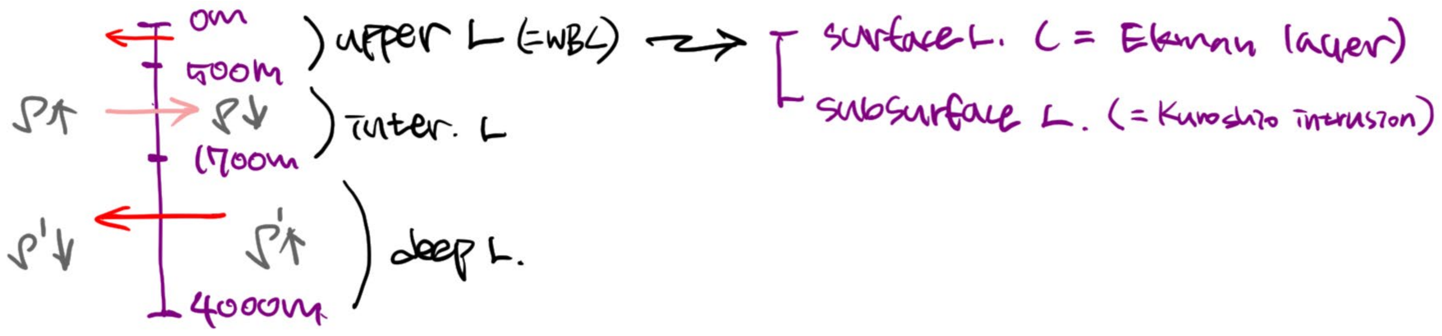

3. 3-layer Sandwiched circulation in SCS

- Monsoon wind
- Kuroshio intrusion

- Luzon strait deepwater overflow

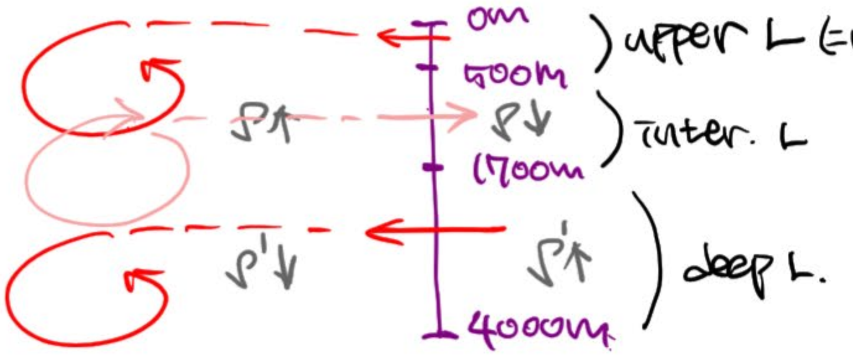

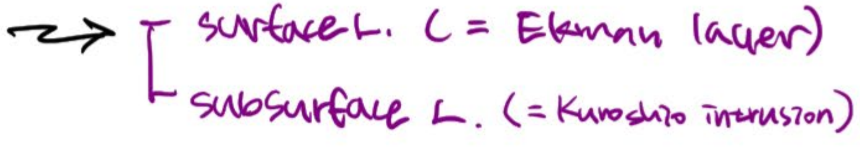

Main drivers

- Surface L: Monsoon wind (directly exposed), Kuroshio intrusion.
- Subsurface L: Kuroshio intrusion (and Monsoon wind)
  - Circulation similar to surface L, but steadier and persistent.

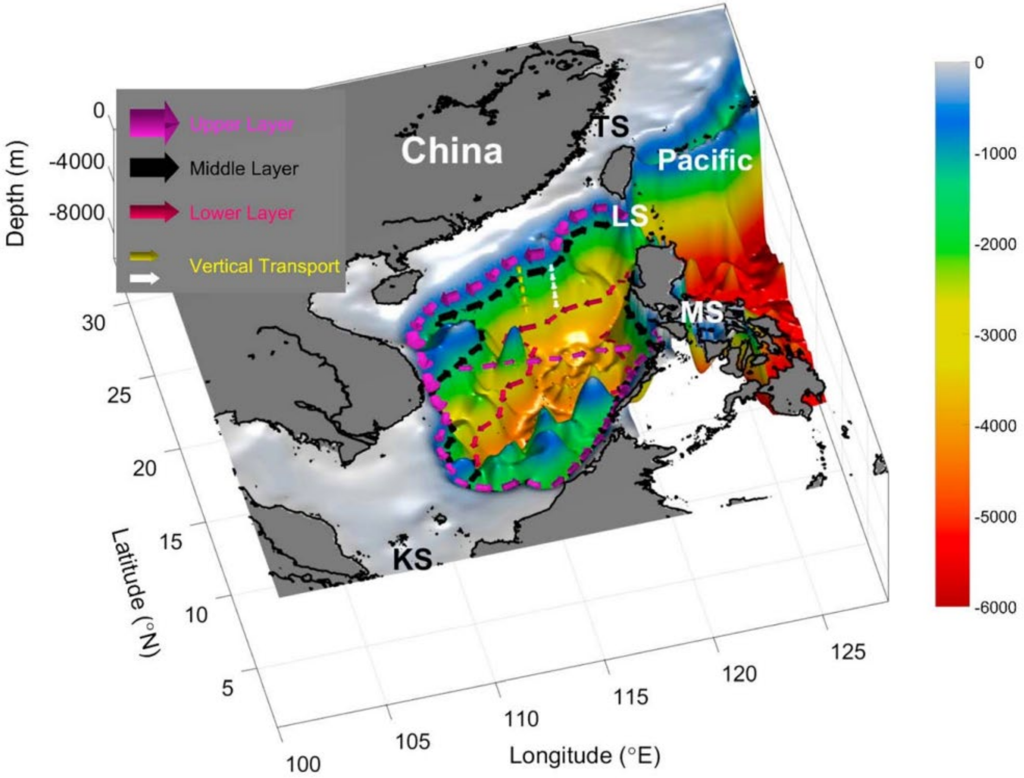

Fig.1 Schematic annual mean CAC circulation, based on Stokes's Theorem [Cai and Gan, 2019].

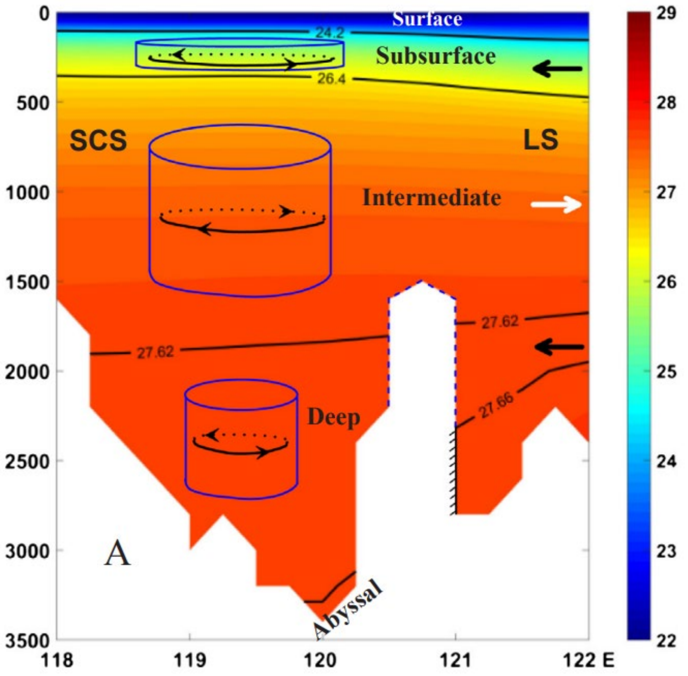

Fig.4 PV flux (thicker arrows) in SCS [Zhu et al., 2019].

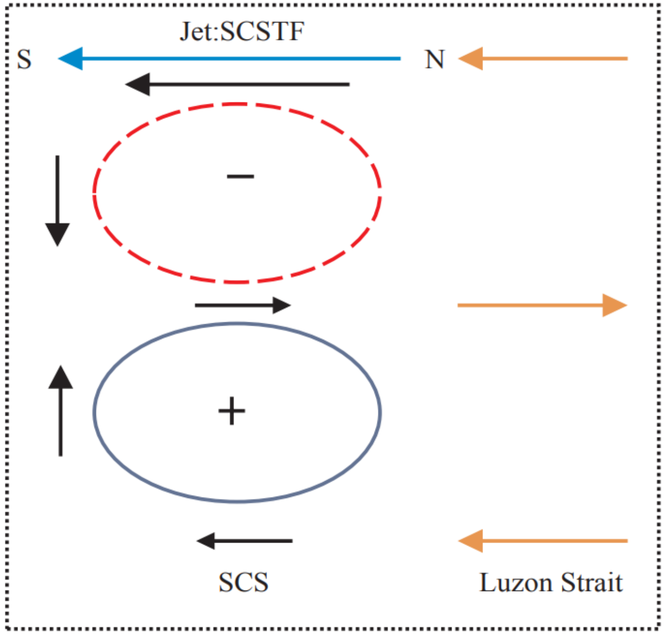

Fig.5 Schematic diagram of the SCS meridional overturning circulation [Wang et al., 2016].

4. ITCZ and monsoon wind

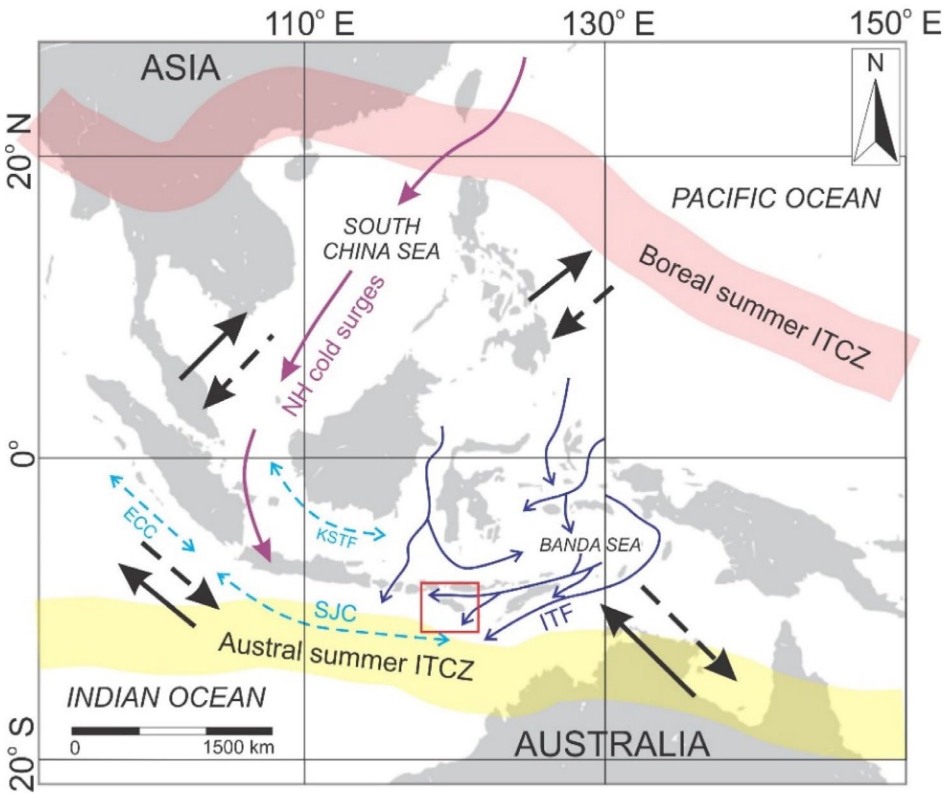

Fig.6 Boreal summer ITCZ (red) and winter ITCZ (yellow) [Ardi et al., 2020].

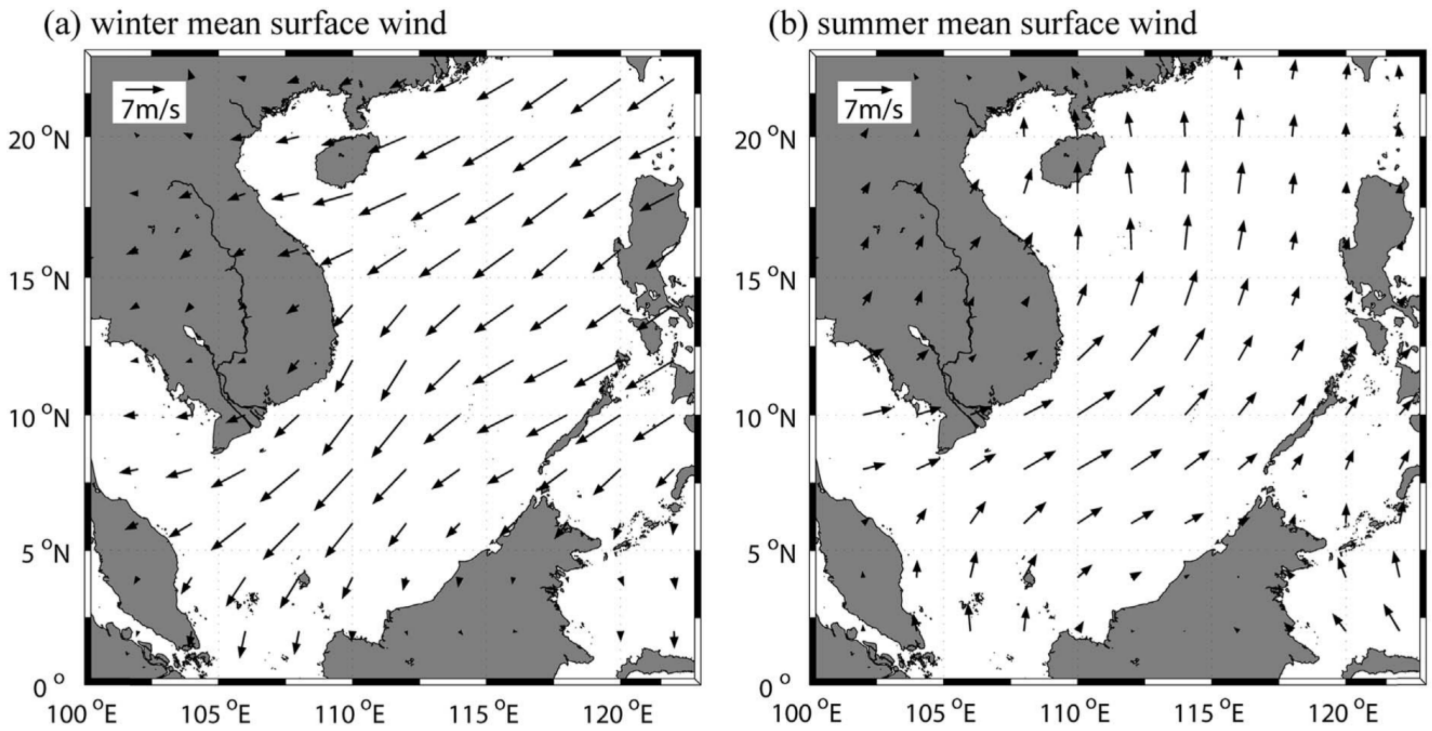

Fig.7 Mean sea surface wind from NOAA-CIRESS 20th C Reanalysis, ver 2 [Park and Choi, 2017].

Weakness

- Ship drift, and hydrographic observations: the issue of sparsity, especially for deeper regions.
- Satellite observations: only provide SSH, SST, SSS.

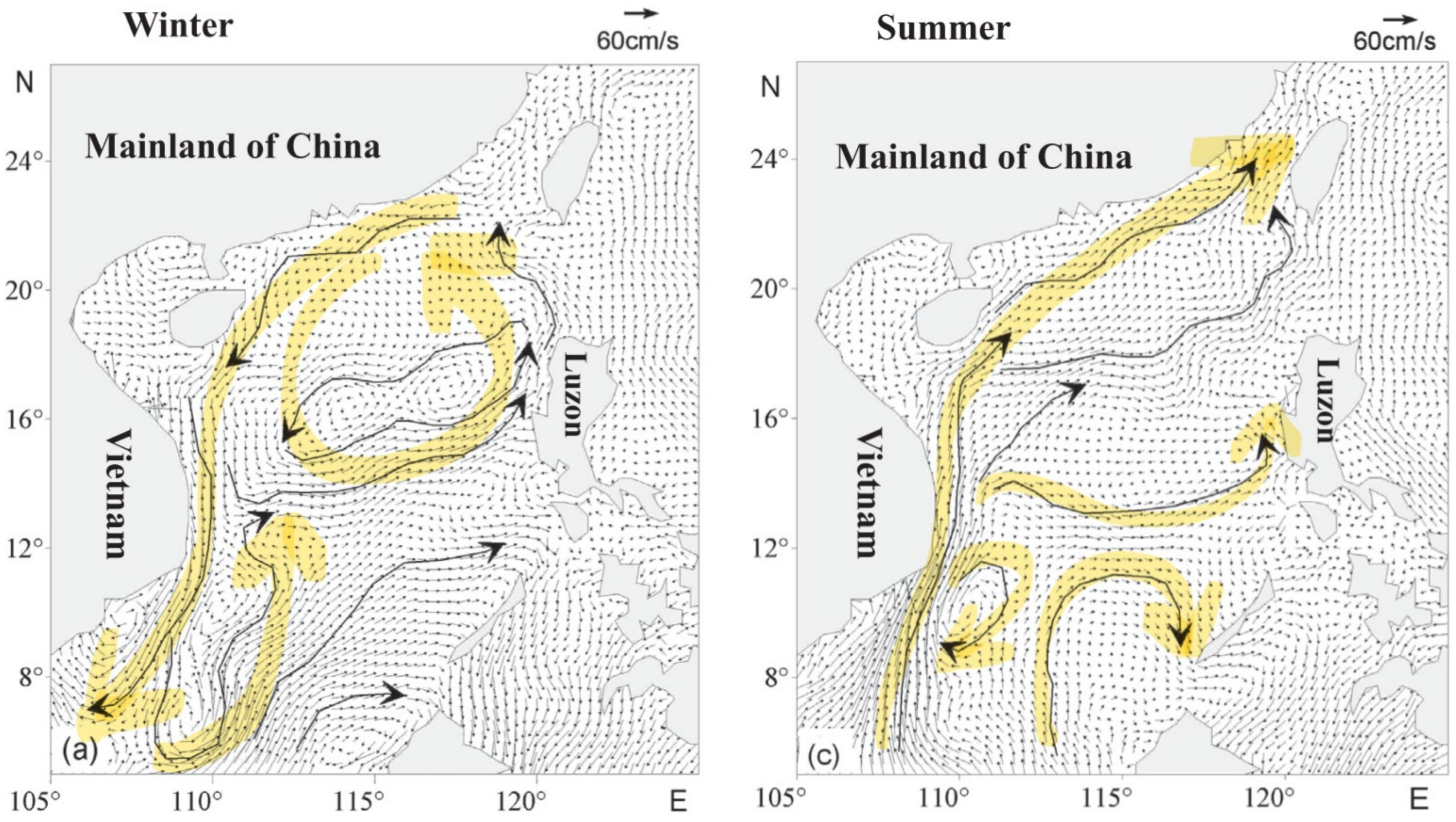

Fig.8 Seasonal mean geostrophic currents at the surface derived from satellite altimetry data [Bao et al., 2005].

Weakness

- Depends on model configuration
  : temporal·spatial resolution, initial conditions, atmospheric forcings, boundary conditions.

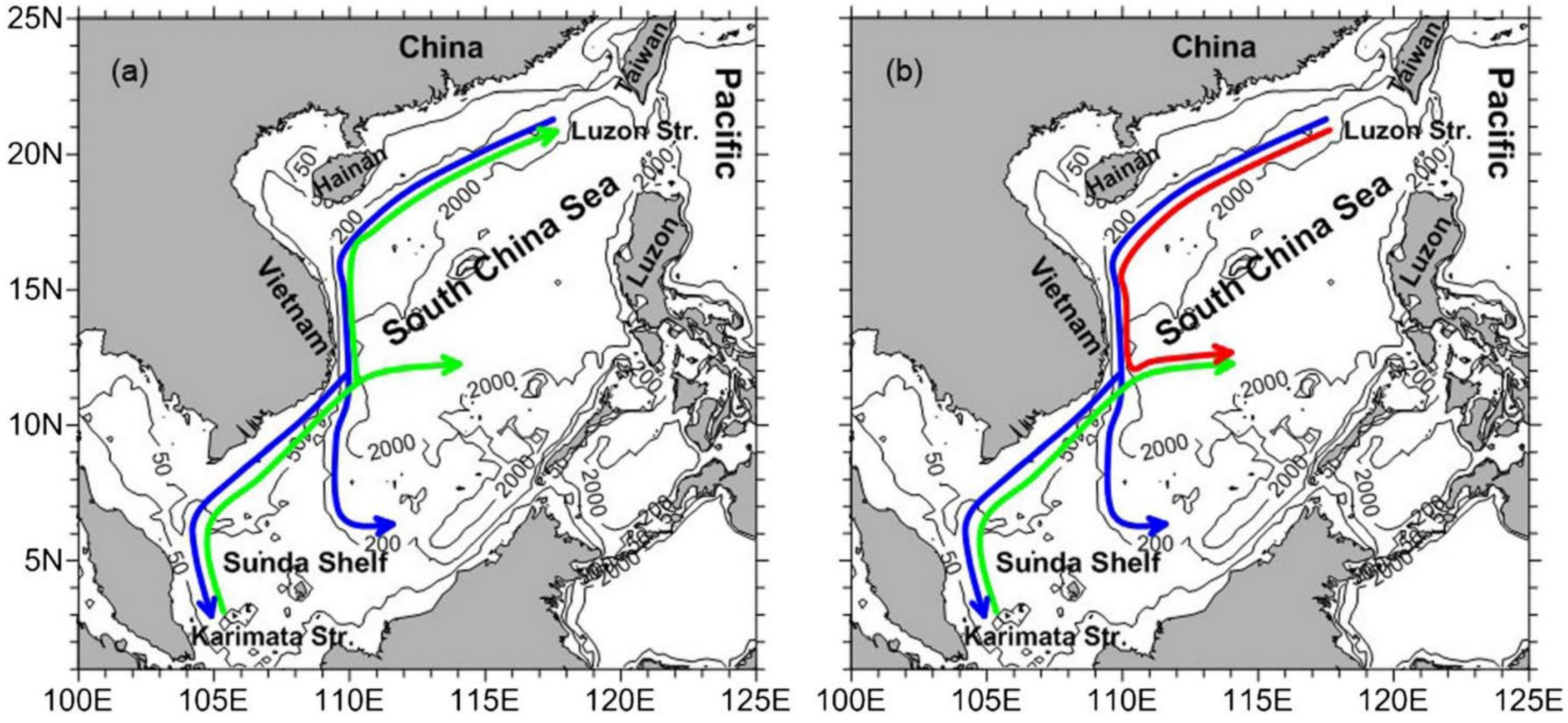

Fig.9 Blue streamline: SCSWBC in winter. (a) Green: SCSWBC in summer in some studies. (b) Green and red: two branches of SCSWBC in summer in some other studies [Quan et al., 2016].

Forward model using MITgcm (before setting up a regional state estimate)

- Bathymetry: GEBCO08+ETOPO
- Artificial walls at the boundaries
- Plain temperature & salinity profiles as initial conditions
- 2 years (1992, 93) of JRA-55 wind forcings

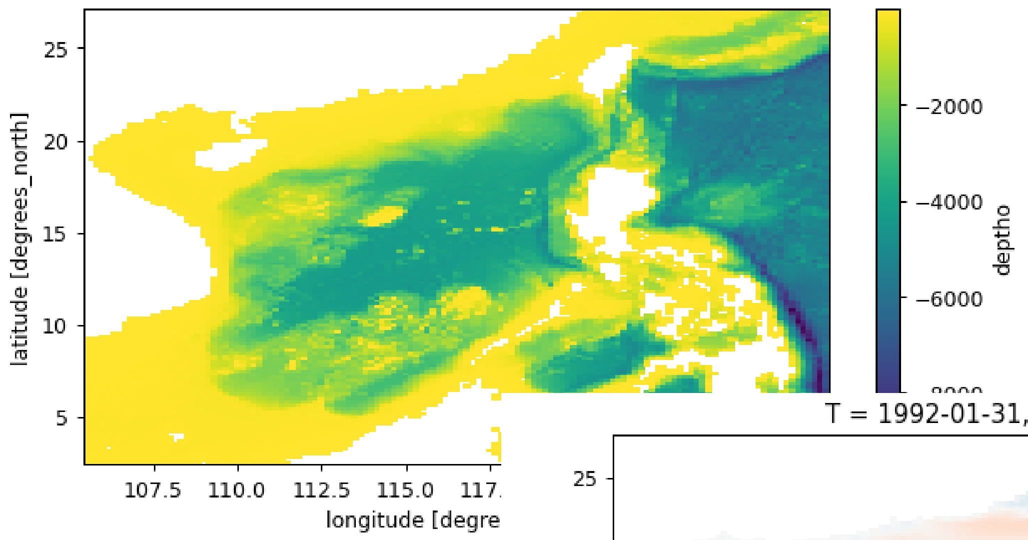

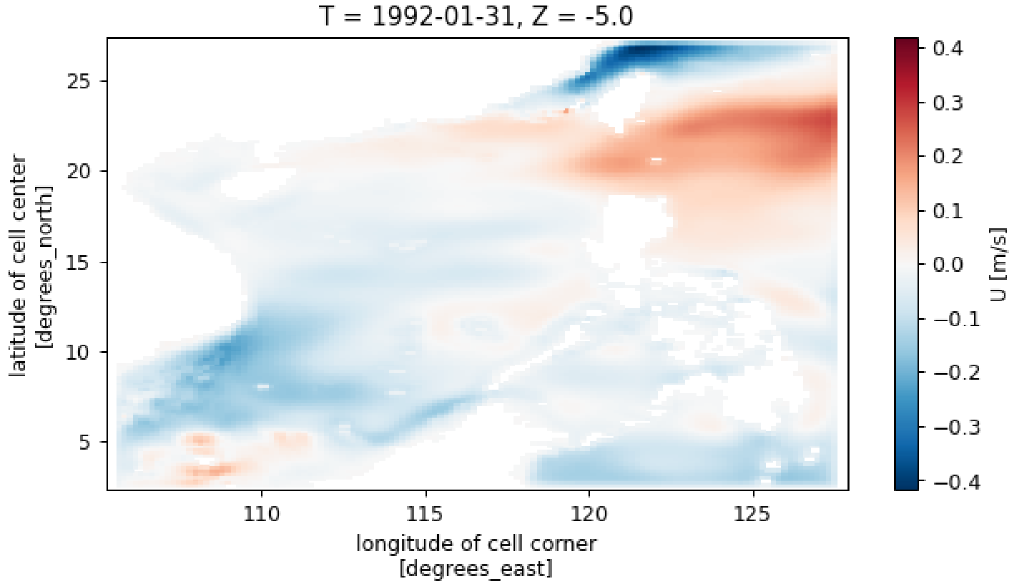

Initial condition

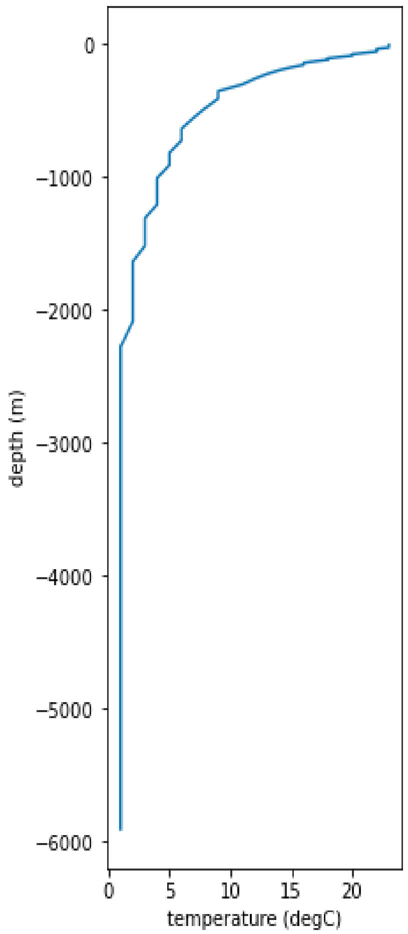

After 2 years

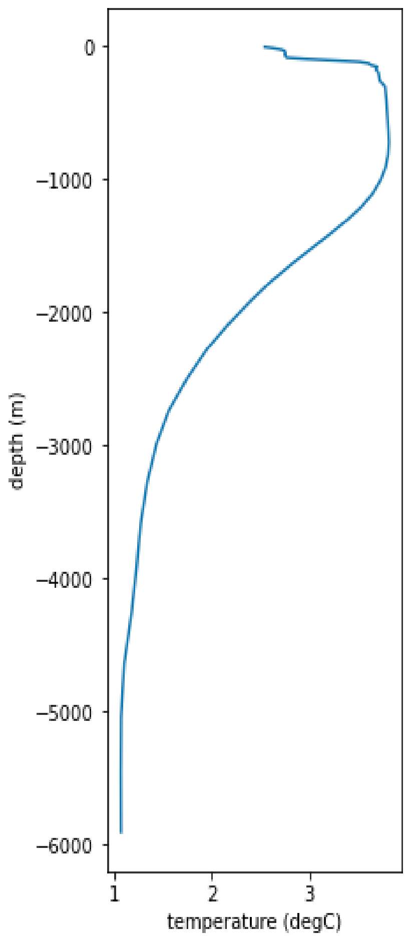

Reference

Ardi, R. D. W., Maryunani, K. A., Yulianto, E., Putra, P. S., & Nugroho, S. H. (2020). Last Deglaciation—Holocene Australian-Indonesian Monsoon Rainfall Changes Off Southwest Sumba, Indonesia. Atmosphere, 11(9), 932.

Cai, Z., & Gan, J. (2019). Coupled external-internal dynamics of layered circulation in the South China Sea: A modeling study. Journal of Geophysical Research: Oceans, 124(7), 5039-5053.

Park, Y. G., & Choi, A. (2017). Long-term changes of South China Sea surface temperatures in winter and summer. Continental Shelf Research, 143, 185-193.

Quan, Q., Xue, H., Qin, H., Zeng, X., & Peng, S. (2016). Features and variability of the South China Sea western boundary current from 1992 to 2011. Ocean Dynamics, 66(6), 795-810.

Wang, D., Xiao, J., Shu, Y., Xie, Q., Chen, J., & Wang, Q. (2016). Progress on deep circulation and meridional overturning circulation in the South China Sea. Science China Earth Sciences, 59(9), 1827-1833.

Xu, F. H., & Oey, L. Y. (2014). State analysis using the Local Ensemble Transform Kalman Filter (LETKF) and the three-layer circulation structure of the Luzon Strait and the South China Sea. Ocean Dynamics, 64(6), 905-923.

Zhu, Y., Sun, J., Wang, Y., Li, S., Xu, T., Wei, Z., & Qu, T. (2019). Overview of the multi-layer circulation in the South China Sea. Progress in oceanography, 175, 171-182.